Editors' Suggestion | Featured in Physics

Run with the Brownian Hare, Hunt with the Deterministic Hounds

Davide Bernardi*
Center for Translational Neurophysiology of Speech and Communication, Fondazione Istituto Italiano di Tecnologia, via Fossato di Mortara 19, 44121 Ferrara, Italy

Benjamin Lindner
Bernstein Center for Computational Neuroscience Berlin, Philippstraße 13, Haus 2, 10115 Berlin, Germany and Physics Department of Humboldt University Berlin, Newtonstraße 15, 12489 Berlin, Germany

(Received 13 October 2021; accepted 24 December 2021; published 26 January 2022)

We present analytic results for mean capture time and energy expended by a pack of deterministic hounds actively chasing a randomly diffusing prey. Depending on the number of chasers, the mean capture time as a function of the prey's diffusion coefficient can be monotonically increasing, decreasing, or attain a minimum at a finite value. Optimal speed and number of chasing hounds exist and depend on each chaser's baseline power consumption. The model can serve as an analytically tractable basis for further studies with bearing on the growing field of smart microswimmers and autonomous robots.

DOI: 10.1103/PhysRevLett.128.040601

A classic textbook problem in differential calculus is finding the trajectory of a dog that runs at a constant speed in the direction of a hare moving in a straight trajectory. Bouguer's solution in 1732 is considered to mark the origin of pursuit theory [1], and mathematical chase-and-escape models have a long tradition in game theory, which has typically focused on optimal evade or pursuit strategies [2–8]. What if, however, the hare's motion is stochastic? Erratic motion could serve as an evasion tactic or, in the microscopic world, it would naturally arise from stochastic interactions with the environment, a case that is particularly interesting since progress in nanotechnology foreshadows the realization of self-propelled particles capable of target pursuit [9–17].

Stochastic elements have been included in optimal-search models on graphs or abstract sets [18–21]; somewhat more realistic yet parsimonious dynamical models that mimic interactions between hunter packs and prey flocks have been proposed [22–29]. Although some of these models include noise terms, they can be studied only through numerical simulations. Considerable analytic efforts were recently devoted to the problem of searching for a fixed target by using stochastic agents or with stochastic resetting [30–43]. Some analytic results exist for models in which a prey that is randomly diffusing on a line [44–46], on grids [47], along graphs [48], or one that adopts a minimal escape strategy [49,50] can bump into random walkers (the "predators"). However, an analytically tractable model in which the predators are actually *chasing* a target that moves randomly in space is missing.

Here, we consider a pack of hounds that pursue a Brownian prey in a d-dimensional space. We first obtain exact solutions for the mean capture time in special cases, which we leverage to derive an analytic approximation that captures the full system's behavior for $d = 2$. In particular, we show that increasing the randomness (the diffusion constant) of the target's trajectory is not necessarily beneficial to escape, unless only one hound is chasing. Furthermore, we find the energetically optimal speed and number of chasers that the hunter should employ: Depending on each chaser's baseline power consumption, the most favorable combination shifts from many slow hounds to fewer and faster hounds.

Model.—The N deterministic hounds move with constant velocity v_0 directly pointing toward the hare, which follows Brownian diffusion. The system obeys

$$\frac{d\boldsymbol{X}}{dt} = \sqrt{2D}\boldsymbol{\xi}(t); \qquad \frac{d\boldsymbol{Y}_n}{dt} = v_0 \frac{\boldsymbol{X} - \boldsymbol{Y}_n}{\|\boldsymbol{X} - \boldsymbol{Y}_n\|}, \tag{1}$$

where $\boldsymbol{X}(t)$ and $\boldsymbol{Y}_n(t)$ indicate the positions of the hare and the nth hound, respectively ($n = 1, \ldots, N$), D sets the diffusion coefficient of the prey, and $\|\cdot\|$ is the Euclidean distance. The d components of the noise vector $\boldsymbol{\xi}(t)$ are Gaussian white noise processes ξ_i with

$$\langle \xi_i \rangle = 0, \qquad \langle \xi_i(t)\xi_j(t') \rangle = \delta_{ij}\delta(t - t'), \tag{2}$$

where angular brackets indicate averaging, δ_{ij} is a Kronecker delta, and $\delta(t - t')$ is a Dirac delta function. At $t = 0$, the hounds are equidistant from each other and $\|\boldsymbol{X}(0) - \boldsymbol{Y}_n(0)\| = \ell$. The hunt terminates whenever any hound comes closer than a prescribed distance $R\ell$ to the target. The capture time (CT) $T_{d,N}$ is a stochastic variable that depends on d and N; it is defined as

$$T_{d,N} = \min\{t | \min_{n=1,\ldots,N}\{\|\boldsymbol{X}(t) - \boldsymbol{Y}_n(t)\|\} \leq R\ell\}. \quad (3)$$

We rescale space and time as follows: $\boldsymbol{x}(t) = \boldsymbol{X}(t)/\ell$, $\boldsymbol{y}_n(t) = \boldsymbol{Y}_n(t)/\ell$, and $\tau = v_0 t/\ell$. By doing so, Eq. (1) becomes [note that $\xi(t) = \sqrt{v_0/\ell}\xi(\tau)$]

$$\frac{d\boldsymbol{x}}{d\tau} = \sqrt{2\hat{D}}\boldsymbol{\xi}(\tau); \qquad \frac{d\boldsymbol{y}_n}{d\tau} = \frac{\boldsymbol{x} - \boldsymbol{y}_n}{\|\boldsymbol{x} - \boldsymbol{y}_n\|}, \quad (4)$$

where $\hat{D} = D/(\ell v_0)$, and $\|\boldsymbol{x}(0) - \boldsymbol{y}_n(0)\| = 1$. In this way, the system is determined by three parameters: the diffusion constant $\hat{D}$, the number of hounds N, and the rescaled capture distance $0 < R < 1$. The rescaled CT will be indicated as $\hat{T}_{d,N}$. In the following, we set $R = 0.1$ and systematically vary $\hat{D}$ and N. Simulation results rely on 10^5 realizations of Eq. (4) per condition using an Euler scheme (time step $\Delta\tau = 10^{-6}$).

One-dimensional case.—In the case $d = 1$, the number of hounds can be at most 2. When $N = 1$, the CT is the first-passage time of a diffusion process with drift across a boundary, a classic problem [51]. In this case, the CT distribution $\rho_1(\tau)$ is the so-called inverse Gaussian [52]. If $N = 2$, the hounds are represented by two absorbing boundaries closing in on the target [Fig. 1(a)]. The distribution of the hare's position can be constructed from a combination of solutions to the free-diffusion equation, chosen such that the moving absorbing boundary conditions are fulfilled [53]. The CT density $\rho_2(\tau)$ is the probability flux through the boundaries [54].

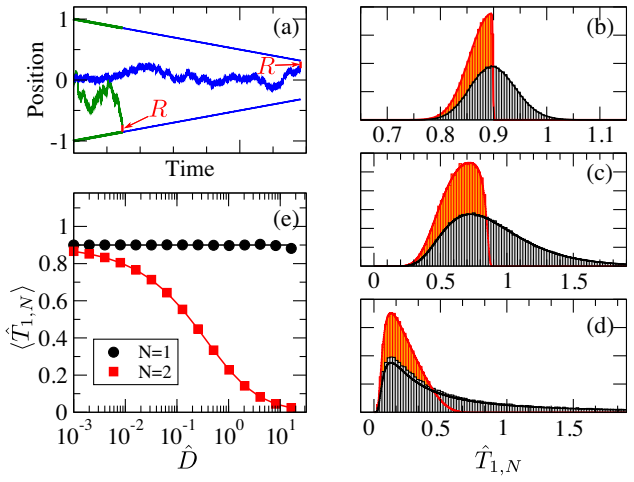

FIG. 1. Hunting a stochastic target on a line. (a) Example trajectories of target and hounds for weak ($\hat{D} = 0.1$, blue lines) and strong ($\hat{D} = 1.0$, green) noise. (b)–(d) Capture time distributions $\rho_1(\tau)$ (black line, theory; gray histogram, simulations) and $\rho_2(\tau)$ (red line, theory; orange histograms, simulations) at three noise levels: (b) $\hat{D} = 0.001$, (c) $\hat{D} = 0.064$, (d) $\hat{D} = 1.024$. (e) Mean CT vs $\hat{D}$ (symbols, simulations; lines, theory).

The CT distributions ρ_1 and ρ_2 are shown in Fig. 1(b) for weak noise intensity; ρ_1 is nearly symmetric, whereas ρ_2 is asymmetric and sharply drops to zero at $\hat{T}_{1,2} = 1 - R$, the time at which the distance between the two hounds falls below $2R$, and thus capture is certain. Increasing the noise level shifts the maximum toward lower values in both cases [Fig. 1(c)]. However, while for $N = 1$ the spread increases, for $N = 2$ a larger noise *decreases* the spread and the distribution takes on a peculiar tilted shape. For strong noise [Fig. 1(d)], ρ_1 is long tailed, while ρ_2 becomes sharply peaked around the maximum, which shifts toward zero. The mean CT when $N = 1$ does not depend on the noise intensity $\langle\rho_1\rangle = 1 - R$ [Fig. 1(e), black line and circles], whereas averaging over ρ_2 yields

$$\langle\hat{T}_{1,2}(\hat{D})\rangle = \hat{D}\left\{\left[\sum_{k=-\infty}^{\infty}(-1)^k\mathcal{B}\left(\frac{1-R}{\hat{D}}, k\right)\right] - 1\right\};$$
$$\mathcal{B}(\alpha, k) = \frac{\alpha(2k-1)^2 + 1 - 2k}{|2k-1|}e^{\alpha k^2}\mathrm{erfc}(\sqrt{\alpha}|k|) - 2\sqrt{\frac{\alpha}{\pi}}, \quad (5)$$

which decreases from $1 - R$ (the deterministic limit) to zero as $\hat{D} \to \infty$ [Fig. 1(e), red line and squares]. The intuitive picture behind these observations is that when $N = 1$ a stronger noise can drive the prey toward the hound or away from it. When $N = 2$, the noise can only move the prey toward either chaser and, therefore, accelerate the capture.

Two-dimensional case.—Moving on to a 2D space, we discuss first the case $N = 1$, which can be solved exactly. To this end, we center the reference frame onto the hound's position $\boldsymbol{y}_1(t)$ and switch to polar coordinates,

$$\boldsymbol{x}(\tau) - \boldsymbol{y}_1(\tau) = \begin{pmatrix} r(\tau)\cos\phi(\tau) \\ r(\tau)\sin\phi(\tau) \end{pmatrix}. \quad (6)$$

In this way, the system's description is determined by the distance between hound and hare $r(\tau) = \|\boldsymbol{x}(\tau) - \boldsymbol{y}_1(\tau)\|$ and the polar angle $\phi(\tau)$. Combining Eqs. (4) and (6) with Itô's lemma yields the following Langevin equations:

$$\frac{d\phi}{d\tau} = \sqrt{2\hat{D}}\xi_\phi(\tau); \qquad \frac{dr}{d\tau} = -1 + \frac{\hat{D}}{r} + \sqrt{2\hat{D}}\xi_r(\tau), \quad (7)$$

in which the noise terms ξ_ϕ and ξ_r obey Eq. (2). The linear term in the equation for r is due to the hound's motion, while the nonlinear term is the Stratonovich drift. The capture condition (3) reduces to $r = R$, which is independent of ϕ. Hence, the CT is the first-passage time through the barrier $r = R$ of a particle starting at $r(0) = \bar{r} = 1$ and diffusing in the potential $\mathcal{U}(r) = r - \hat{D}\ln(r)$. The known quadrature formula [55] yields the exact elementary solution for the mean CT

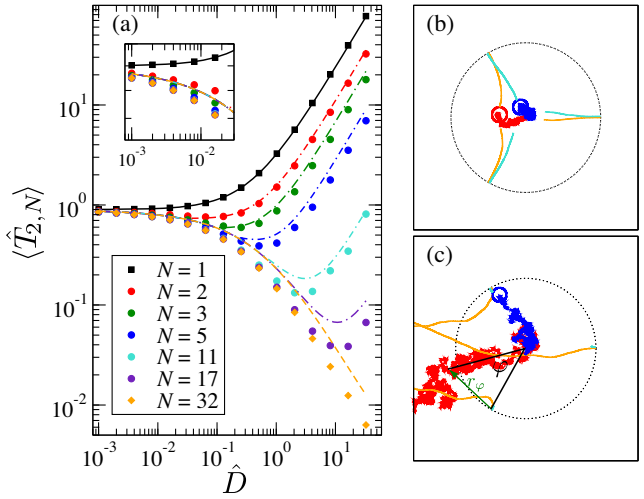

FIG. 2. Hunting a stochastic target in 2D, seen from the target's perspective. (a) Mean CT as a function of $\hat{D}$ for different values of N [symbols, simulations as in the legend; black solid line, theory (8); orange dashed line, theory (5); dash-dotted lines, theory (9) with Eq. (5) as lower bound, see text]. Inset: close-up of small $\hat{D}$ range. (b) Two realizations for $N = 3$ and weak noise ($\hat{D} = 0.01$). (c) Same for strong noise ($\hat{D} = 1$). Exit angle φ and initial pursuit distance r_φ of the escaped trajectory are indicated. For this trajectory, capture occurs outside the shown area.

$$\langle \hat{T}_{2,1}(\bar{r}, \hat{D}) \rangle = \frac{1}{\hat{D}} \int_R^{\bar{r}} dy \frac{e^{y/\hat{D}}}{y} \int_y^\infty dz z e^{-z/\hat{D}} = \bar{r} - R + \hat{D} \ln\left(\frac{\bar{r}}{R}\right), \quad (8)$$

where a generic starting distance $\bar{r}$ is kept for later convenience. Figure 2(a) shows Eq. (8) with $\bar{r} = 1$ (solid black line) together with simulations (black circles). Because the potential $\mathcal{U}(r)$ has a minimum at $r = \hat{D}$, only the linear part matters if $\hat{D} \ll R$. In this case, the CT distribution is similar to the inverse Gaussian $\rho_1(\tau)$; indeed, $\langle \hat{T}_{2,1}(\hat{D}) \rangle$ is nearly constant in the left part of Fig. 2(a). For larger noise ($\hat{D} > R$), the potential creates an escape barrier $\Delta\mathcal{U} = \hat{D} \ln(\hat{D}/R) + R - \hat{D}$, which is an increasing function of $\hat{D}$, thus causing $\langle \hat{T}_{2,1}(\hat{D}) \rangle$ to increase monotonically.

When $N \geq 2$, the hounds start at evenly spaced angles on the unit circle [dotted line in Figs. 2(b) and 2(c)]. During the hunt, however, the target diffuses away from the origin so that the circular symmetry is lost (the hounds are effectively coupled through the target). In the weak-noise limit, however, the hare's typical displacement from the origin is small when it is reached by the hounds, which act as a tightening noose [Fig. 2(b)]. Hence, the mean CT depends weakly on N for $N \geq 2$ and small $\hat{D}$, as simulations demonstrate [circles and diamonds in Fig. 2(a), close-up in the inset]. Considering the distance to the nearest hound and neglecting the angular diffusion suggests that $\langle \hat{T}_{2,N\geq 2}(\hat{D}) \rangle \approx \langle \hat{T}_{1,2}(\hat{D}) \rangle$. Figure 2(a) shows that Eq. (5), the theory for $d = 1$, $N = 2$ (orange dashed line), is indeed close to simulations for small $\hat{D}$.

In the strong-noise limit, the hare's diffusive motion rapidly covers much longer distances than the hounds, which barely move from their starting position as the hare typically reaches the unit circle for the first time. We distinguish two cases: (i) "ensnared" trajectories, if the hare hits a hound inside the unit circle [Fig. 2(c), blue trajectory] and (ii) "escaped" trajectories, along which the hare slips through and diffuses away [Fig. 2(c), red trajectory], chased by the hounds [Fig. 2(c), orange trajectories]. If the Stratonovich drift is ignored, the mean CT of the ensnared ensemble can be approximated by Eq. (5). The actual mean CT is slightly smaller because the neglected term drives the prey mostly toward the hounds. If the prey exits the ring, the hounds tend to group together during the pursuit, and we can argue that the closest hound matters the most. Hence, we approximate the mean CT by using Eq. (8) with initial distance $\bar{r} = r_\varphi = \sqrt{R^2 + 2(1+R)(1-\cos\varphi)}$, the distance from a point on the circle of radius $1 + R$ to the nearest hound, which depends on the hare's exit angle φ [Fig. 2(c)]. Because a large noise fluctuation can shove the target toward a different hound, except for the closest upon exit from the unit circle, this approximation tends to overestimate the CT. Averaging over ensnared and escaped trajectories yields

$$\langle \hat{T}_{2,N}(\hat{D}) \rangle \approx p_N \langle\langle \hat{T}_{2,1}(r_\varphi, \hat{D}) \rangle\rangle_\varphi + (1 - p_N) \langle \hat{T}_{1,2}(\hat{D}) \rangle, \quad (9)$$

where p_N is the fraction of escaped trajectories, and we assume a uniform distribution in the interval $(0, \pi/N)$ to average over φ [56]. To estimate p_N, we first note that in the limit $\hat{D} \to \infty$ the hounds do not move, and that p_N is the fraction of trajectories that start from the origin and reach the ring of radius $1 + R$ without hitting one of the motionless hounds beforehand. Suppose p_1 is known. If the N hounds are sufficiently spaced, we make the rough approximation that the probability of going from one hound to another one before hitting the exit boundary is $1 - p_1$, which leads to $p_N \approx p_1^N$. Computing p_1 exactly is hard due to the lack of circular symmetry. If, however, the exit boundary is replaced by a circle of radius $2 + R$ centered on the static hound, the exact solution $p_{\text{lb}} = \ln(R)/\ln[R/(2+R)]$ is known [57]. Since the new boundary encompasses the original one, p_{lb} is a lower bound for p_1. Taking $p_1 \approx p_{\text{lb}}$ and combining with the above argument gives $p_N \approx \{\ln(R)/\ln[R/(2+R)]\}^N$. We remark that this approximation is only valid for strong noise, and it also fails when N becomes large. In particular, when N approaches the value $N_{\max} = \lceil \pi/\arcsin R \rceil$, the spacing between the hounds' starting positions is so small that the ring is effectively inescapable ($p_{N \geq N_{\max}} = 0$). As a way to

make Eq. (9) work also for the weak-noise range, we set $p_N = 0$ whenever the right-hand side of Eq. (9) falls below $\langle \hat{T}_{1,2}(\hat{D})\rangle$. Note that when $p_N = 0$, Eq. (9) reduces to the weak-noise approximation (5). With this choice, the qualitative picture is well captured by the theory over the entire range of $\hat{D}$, and even the quantitative agreement is satisfactory, as seen in Fig. 2(a).

Remarkably, the mean CT attains a minimum at a finite $\hat{D}$ for every N except $N = 1$ and $N = N_{\max} = 32$. Therefore, increasing the prey's diffusion constant is, on average, beneficial to escape only above some "critical" noise level. When $N = 1$ or $N = N_{\max}$, a stronger noise always delays or accelerates the capture, respectively. These two monotonic courses, which are analogous to escaped and ensnared trajectories, respectively, are weighted according to Eq. (9) when $1 < N < N_{\max}$. Hence, a minimum comes about. Adding more chasers changes the weighting factor p_N and thus shifts the minimum's position toward higher $\hat{D}$.

The hunter's perspective.—We now switch the viewpoint, reintroduce the hounds' speed v_0, and revert to the original time units $t = \tau \ell v_0^{-1}$. The mean CT as a function of v_0 is $\langle T_{2,N}(v_0)\rangle = \ell v_0^{-1}\langle \hat{T}_{2,N}[D/(\ell v_0)]\rangle$, shown in Fig. 3(a) (here, $D = \ell = 1$). Intuitively, the mean CT is a decreasing function of v_0 for all N—faster hounds capture the target more rapidly. At large v_0, all curves converge to the deterministic limit $\langle T_{2,N}\rangle \sim \ell(1-R)/v_0$. When $v_0 \to 0$, only trapped trajectories give a finite contribution to the mean CT; the mean CT of escaped trajectories is infinite, so that the mean CT always diverges, except for $N = N_{\max}$.

From the hunter's perspective, possibly more relevant than the mean CT is the energy spent by the hounds to capture the prey. Assuming that dissipation is due to a drag force $\boldsymbol{F} = -\gamma d\boldsymbol{Y}_n/dt$, the expended energy is

$$\langle E_N\rangle = \left\langle \sum_{n=1}^{N} \int d\boldsymbol{Y}_n \cdot \gamma \frac{d\boldsymbol{Y}_n}{dt} \right\rangle = N\gamma v_0^2 \langle T_{2,N}\rangle, \qquad (10)$$

which is shown in Fig. 3(b) (here $\gamma = 1$). For all values of N, $\langle E_N\rangle$ is an increasing function of v_0. Remarkably, all curves roughly intersect at $v_0 \approx D = 1$, which means that the expended energy is essentially independent of the number of employed hounds (although capture is faster for larger N). At greater v_0, $\langle E_N\rangle$ grows with the number of hounds and for $v_0 \to \infty$ it is proportional to the speed and number of hounds $\langle E_N\rangle \sim N\ell v_0(1-R)$; because the mean CT does not depend much on N, it is more efficient to employ one hound. The situation is reversed when hounds are slow. In the limit $v_0 \to 0$, the consumed energy is $\langle E_1\rangle \to D\ln(1/R)$ for a single hound. For $2 \le N < N_{\max}$, $\langle E_N\rangle \sim N p_1^N D\langle \ln(r_\varphi/R)\rangle_\varphi$, which is a decreasing function of N (note that the average over φ drops with N). Finally, $E_{N_{\max}}(v_0 \to 0) \to 0$.

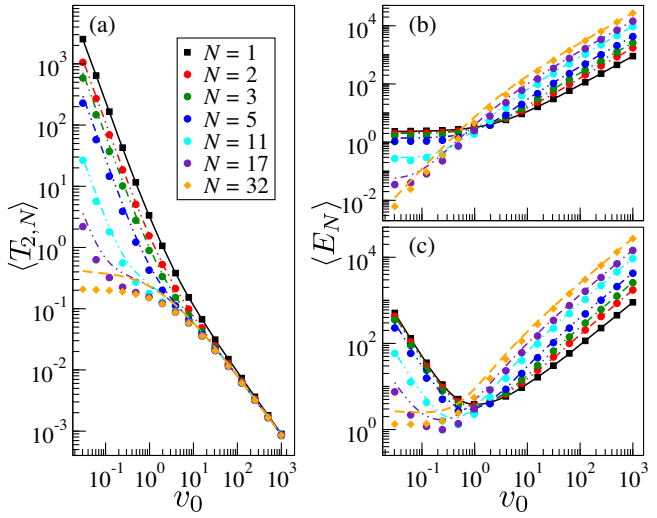

FIG. 3. Hunter's perspective. (a) Mean CT as a function of v_0 for different N (see legend). (b) Mean dissipated energy with purely linear drag, see Eq. (10). (c) Same as (b), with additional "metabolic" penalty, see Eq. (11). Line, symbol, and color coding as in Fig. 2(a).

Altogether, Fig. 3(b) suggests that the most energy efficient way is to employ many slow hounds. Except for the somewhat forced case of $N = N_{\max}$, however, the mean CT diverges for $v_0 \to 0$, which makes this limit theoretically curious, but of little practical relevance. It is natural to introduce a constant power consumption β that is independent of the hound's motion and that models the baseline metabolism or power drain necessary to keep each hound functional. With this additional term, Eq. (10) becomes

$$\langle E_N\rangle = N(\gamma v_0^2 + \beta)\langle T_{2,N}\rangle. \qquad (11)$$

Figure 3(c) shows how the results of Fig. 3(b) are changed by the additional term (here $\beta = 0.2$). The energetic cost of a slow CT is increased, so that for each N a minimum (an optimal v_0) appears. Furthermore, the global minimum is now at a finite value of v_0. The optimal v_0 and N depend on β (increasing β shifts v_0 toward larger values and pushes N toward smaller numbers).

Conclusion.—In this Letter, we proposed a stochastic extension of the problem that originated pursuit theory. This model is simple enough to make an analytic characterization possible, but shows a rich collection of phenomena. For instance, the behavior of the mean CT as a function of the prey's diffusivity can be, depending on the number of chasers, strictly increasing, decreasing, or nonmonotonic. In this last case, a critical noise level could be defined, above which the mean CT becomes larger than in the deterministic case. From the hunter's perspective, we found how the most efficient speed and number of hounds depends on each hound's "baseline metabolism."

Concerning the only parameter that was not systematically varied, the system's behavior for other values of R is qualitatively similar, provided that $\hat{D}$ and N are scaled accordingly (not shown). Equation (9) still applies, although the approximation for p_N discussed above becomes less accurate for values of R that are close to either 0 or 1, which describe the less interesting situation of exceedingly small or large targets.

The pursuit model analyzed here is idealized, but it could portray, for instance, a situation in which a randomly moving target is chased by autonomous or remote-controlled robots [58–62]. A further scenario the model could represent is that of microswimmers that exhibit chemotacticlike behavior [63–66], if chemical signals travel fast and chasers are subject to a much weaker noise than the target. We envision many possible model variations that should describe more elaborate situations, while preserving mathematical tractability, such as a random starting position for the chasers, the case $d = 3$, an external field, a drift term for the prey, or a stochastic term for the chasers' velocity.

B. L. would like to thank Peter J. Thomas for his hospitality at Case Western Reserve University, where a first idea for this work was conceived. We would also like to acknowledge David Papo for useful comments on the draft of this article.

*davide.bernardi@iit.it, davide.bernardi@bccn-berlin.de

[1] P. J. Nahin, *Chases and Escapes: The Mathematics of Pursuit and Evasion* (Princeton University Press, Princeton, NJ, 2007).
[2] R. Isaacs, *Differential games. A Mathematical Theory with Applications to Warfare and Pursuit, Control and Optimization* (Wiley, New York, 1965).
[3] B. Halpern, The robot and the rabbit—a pursuit problem, Am. Math Mon. **76**, 140 (1969).
[4] J. G. Foreman, Differential search games with mobile hider, SIAM J. Control Optim. **15**, 841 (1977).
[5] C. H. Fitzgerald, The princess and monster differential game, SIAM J. Control Optim. **17**, 700 (1979).
[6] S. Gal, On the optimality of a simple strategy for searching graphs, Int. J. Game Theory **29**, 533 (2001).
[7] G. Owen and G. H. McCormick, Finding a moving fugitive. A game theoretic representation of search, Computers and Operations Research **35**, 1944 (2008).
[8] S. Alpern, R. Fokkink, R. Lindelauf, and G.-J. Olsder, The "princess and monster" game on an interval, SIAM J. Control Optim. **47**, 1178 (2008).
[9] R. Golestanian, T. B. Liverpool, and A. Ajdari, Propulsion of a Molecular Machine by Asymmetric Distribution of Reaction Products, Phys. Rev. Lett. **94**, 220801 (2005).
[10] Y. Hong, N. M. K. Blackman, N. D. Kopp, A. Sen, and D. Velegol, Chemotaxis of Nonbiological Colloidal Rods, Phys. Rev. Lett. **99**, 178103 (2007).
[11] L. Zhang, J. Abbott, L. Dong, B. Kratochvil, D. Bell, and B. Nelson, Artificial bacterial flagella: Fabrication and magnetic control, Appl. Phys. Lett. **94**, 064107 (2009).
[12] S. Sengupta, M. E. Ibele, and A. Sen, Fantastic voyage: Designing self-powered nanorobots, Angew. Chem., Int. Ed. **51**, 8434 (2012).
[13] M. You, C. Chen, L. Xu, F. Mou, and J. Guan, Intelligent micro/nanomotors with taxis, Acc. Chem. Res. **51**, 3006 (2018).
[14] M. N. Popescu, W. E. Uspal, C. Bechinger, and P. Fischer, Chemotaxis of active Janus nanoparticles, Nano Lett. **18**, 5345 (2018).
[15] S. Palagi and P. Fischer, Bioinspired microrobots, Nat. Rev. Mater. **3**, 113 (2018).
[16] M. Medina-Sénchez, V. Magdanz, M. Guix, V. Fomin, and O. Schmidt, Swimming microrobots: Soft, reconfigurable, and smart, Adv. Funct. Mater. **28**, 1707228 (2018).
[17] L. Alvarez, M. Fernandez-Rodriguez, and A. Alegria, Reconfigurable artificial microswimmers with internal feedback, Nat. Commun. **12**, 4762 (2021).
[18] J. M. Dobbie, Search for an avoiding target, SIAM J. Appl. Math. **28**, 72 (1975).
[19] P. Bernhard, A.-L. Colomb, and G. P. Papavassilopoulos, Rabbit and hunter game: Two discrete stochastic formulations, Comput. Math. Appl. **13**, 205 (1987).
[20] A. Bonato, D. Mitsche, X. Pérez-Giménez, and P. Prałat, A probabilistic version of the game of zombies and survivors on graphs, Theor. Comput. Sci. **655**, 2 (2016).
[21] F. Simard, J. Desharnais, and F. Laviolette, General cops and robbers games with randomness, Theor. Comput. Sci. **887**, 30 (2021).
[22] R. Vidal, O. Shakernia, H. J. Kim, D. H. Shim, and S. Sastry, Probabilistic pursuit-evasion games: Theory, implementation, and experimental evaluation, IEEE Transactions on Robotics and Automation **18**, 662 (2002).
[23] P. Romanczuk, I. D. Couzin, and L. Schimansky-Geier, Collective Motion due to Individual Escape and Pursuit Response, Phys. Rev. Lett. **102**, 010602 (2009).
[24] A. Kamimura and T. Ohira, Group chase and escape, New J. Phys. **12**, 053013 (2010).
[25] L. Angelani, Collective Predation and Escape Strategies, Phys. Rev. Lett. **109**, 118104 (2012).
[26] T. Iwama and M. Sato, Group chase and escape with some fast chasers, Phys. Rev. E **86**, 067102 (2012).
[27] Y. Lin and N. Abaid, Collective behavior and predation success in a predator-prey model inspired by hunting bats, Phys. Rev. E **88**, 062724 (2013).
[28] M. Janosov, C. Virágh, G. Vásárhelyi, and T. Vicsek, Group chasing tactics: How to catch a faster prey, New J. Phys. **19**, 053003 (2017).
[29] A. Surendran, M. Plank, and M. Simpson, Spatial structure arising from chase-escape interactions with crowding, Sci. Rep. **9**, 14988 (2019).
[30] M. A. Lomholt, T. Ambjörnsson, and R. Metzler, Optimal Target Search on a Fast-Folding Polymer Chain with Volume Exchange, Phys. Rev. Lett. **95**, 260603 (2005).
[31] G. Oshanin, H. S. Wio, K. Lindenberg, and S. F. Burlatsky, Intermittent random walks for an optimal search strategy: One-dimensional case, J. Phys. Condens. Matter **19**, 065142 (2007).

[32] M. R. Evans and S. N. Majumdar, Diffusion with Stochastic Resetting, Phys. Rev. Lett. **106**, 160601 (2011).

[33] C. Mejía-Monasterio, G. Oshanin, and G. Schehr, First passages for a search by a swarm of independent random searchers, J. Stat. Mech. (2011) P06022.

[34] L. Kusmierz, S. N. Majumdar, S. Sabhapandit, and G. Schehr, First Order Transition for the Optimal Search Time of Lévy Flights with Resetting, Phys. Rev. Lett. **113**, 220602 (2014).

[35] V. V. Palyulin, A. V. Chechkin, and R. Metzler, Lévy flights do not always optimize random blind search for sparse targets, Proc. Natl. Acad. Sci. U.S.A. **111**, 2931 (2014).

[36] A. Pal and S. Reuveni, First Passage under Restart, Phys. Rev. Lett. **118**, 030603 (2017).

[37] A. Falcón-Cortés, D. Boyer, L. Giuggioli, and S. N. Majumdar, Localization Transition Induced by Learning in Random Searches, Phys. Rev. Lett. **119**, 140603 (2017).

[38] A. Pezzotta, M. Adorisio, and A. Celani, Chemotaxis emerges as the optimal solution to cooperative search games, Phys. Rev. E **98**, 042401 (2018).

[39] J. Noetel, V. L. S. Freitas, E. E. N. Macau, and L. Schimansky-Geier, Optimal noise in a stochastic model for local search, Phys. Rev. E **98**, 022128 (2018).

[40] A. Chechkin and I. M. Sokolov, Random Search with Resetting: A Unified Renewal Approach, Phys. Rev. Lett. **121**, 050601 (2018).

[41] G. Mercado-Vásquez and D. Boyer, First Hitting Times to Intermittent Targets, Phys. Rev. Lett. **123**, 250603 (2019).

[42] M. R. Shaebani, R. Jose, L. Santen, L. Stankevicins, and F. Lautenschläger, Persistence-Speed Coupling Enhances the Search Efficiency of Migrating Immune Cells, Phys. Rev. Lett. **125**, 268102 (2020).

[43] M. Dahlenburg, A. V. Chechkin, R. Schumer, and R. Metzler, Stochastic resetting by a random amplitude, Phys. Rev. E **103**, 052123 (2021).

[44] P. L. Krapivsky and S. Redner, Kinetics of a diffusive capture process: Lamb besieged by a pride of lions, J. Phys. A **29**, 5347 (1996).

[45] K. Winkler and A. J. Bray, Drowsy cheetah hunting antelopes: A diffusing predator seeking fleeing prey, J. Stat. Mech. (2005) P02005.

[46] A. Gabel, S. N. Majumdar, N. K. Panduranga, and S. Redner, Can a lamb reach a haven before being eaten by diffusing lions?, J. Stat. Mech. (2012) P05011.

[47] J. Peng and E. Agliari, First encounters on combs, Phys. Rev. E **100**, 062310 (2019).

[48] T. Weng, J. Zhang, M. Small, and P. Hui, Hunting for a moving target on a complex network, Europhys. Lett. **119**, 48006 (2017).

[49] G. Oshanin, O. Vasilyev, P. L. Krapivsky, and J. Klafter, Survival of an evasive prey, Proc. Natl. Acad. Sci. U.S.A. **106**, 13696 (2009).

[50] M. Schwarzl, A. Godec, G. Oshanin, and R. Metzler, A single predator charging a herd of prey: Effects of self volume and predator–prey decision-making, J. Phys. A **49**, 225601 (2016).

[51] E. Schrödinger, Zur Theorie der Fall- und Steigversuche an Teilchen mit Brownscher Bewegung, Phys. Z. **16**, 289 (1915).

[52] The inverse Gaussian distribution is $\rho_1(\tau) = \exp[-(1-R-\tau)^2/(4\tau)]/\sqrt{4\pi\tau^3}$.

[53] The distribution of the hare's position $P_2(x,\tau)$ must satisfy the diffusion equation with absorbing boundary conditions at the hounds' positions $a_\pm(\tau) = \pm(x_c - \tau)$, where $x_c = 1 - R$. We make the ansatz $P_2(x,\tau) = P_{2,0}(x,\tau) + \sum_{k=1}^{\infty}(-1)^k[P^+_{2,k}(x,\tau) + P^-_{2,k}(x,\tau)]$, where $P^\pm_{2,k}(x,\tau) = \exp[x_c\lambda_k/\hat{D} - (x \mp \kappa_k x_c)^2/(4\hat{D}\tau)]/\sqrt{4\pi\hat{D}\tau}$ solves the free-diffusion equation, and κ_k and λ_k are integers such that $P^\pm_{2,k+1}(a_\pm(\tau),\tau) = P^\mp_{2,k}(a_\pm(\tau),\tau)$. Imposing this condition leads to the recursion relations $\kappa_0 = \lambda_0 = 0$; $\kappa_{k+1} = \kappa_k + 2; \lambda_{k+1} = \lambda_k + \kappa_k + 1$, which are solved by $\kappa_k = 2k, \lambda_k = k^2$. With this choice, the boundary conditions are fulfilled, i.e., $P_2(a_\pm(\tau),\tau) = 0$.

[54] For symmetry, the total probability flux is twice the flux through either boundary $-2\hat{D}\partial/\partial x P_2(x,\tau)|_{x=a_+(\tau)}$, from which one finds $\rho_2(\tau) = \sum_{k=0}^{\infty}(2-\delta_{0k})(-1)^k/(16\pi\hat{D}\tau^3)^{1/2} \times \exp(x_c k^2/\hat{D})[\mathcal{G}(-k) + \mathcal{G}(k)]$, where $\mathcal{G}(k) = [x_c(1+2k) - \tau] \times \exp[-[x_c(1+2k) - \tau]^2/(4\hat{D}\tau)]$.

[55] C. W. Gardiner, *Handbook of Stochastic Methods* (Springer-Verlag, Berlin, 1985).

[56] Angular diffusion and absorbing boundary make this approximation not so accurate, especially for large N.

[57] J. G. Wendel, Hitting spheres with Brownian motion, Ann. Probab. **8**, 164 (1980).

[58] C. Stefanini, S. Orofino, L. Manfredi, S. Mintchev, S. Marrazza, T. Assaf, L. Capantini, E. Sinibaldi, S. Grillner, P. Wallén, and P. Dario, A novel autonomous, bioinspired swimming robot developed by neuroscientists and bioengineers, Bioinspiration Biomimetics **7**, 025001 (2012).

[59] M. Brambilla, E. Ferrante, M. Birattari, and M. Dorigo, Swarm robotics: A review from the swarm engineering perspective, Swarm Intell. **7**, 1 (2013).

[60] M. Duarte, V. Costa, J. Gomes, T. Rodrigues, F. Silva, S. M. Oliveira, and A. L. Christensen, Evolution of collective behaviors for a real swarm of aquatic surface robots, PLoS One **11**, 1 (2016).

[61] M. Karásek, F. T. Muijres, C. D. Wagter, B. D. W. Remes, and G. C. H. E. de Croon, A tailless aerial robotic flapper reveals that flies use torque coupling in rapid banked turns, Science **361**, 1089 (2018).

[62] G. Wang, T. V. Phan, S. Li, M. Wombacher, J. Qu, Y. Peng, G. Chen, D. I. Goldman, S. A. Levin, R. H. Austin, and L. Liu, Emergent Field-Driven Robot Swarm States, Phys. Rev. Lett. **126**, 108002 (2021).

[63] B. M. Friedrich and F. Jülicher, Chemotaxis of sperm cells, Proc. Natl. Acad. Sci. U.S.A. **104**, 13256 (2007).

[64] B. M. Friedrich and F. Jülicher, Steering Chiral Swimmers along Noisy Helical Paths, Phys. Rev. Lett. **103**, 068102 (2009).

[65] P. K. Ghosh, Y. Li, F. Marchesoni, and F. Nori, Pseudo-chemotactic drifts of artificial microswimmers, Phys. Rev. E **92**, 012114 (2015).

[66] H. D. Vuijk, H. Merlitz, M. Lang, A. Sharma, and J.-U. Sommer, Chemotaxis of Cargo-Carrying Self-Propelled Particles, Phys. Rev. Lett. **126**, 208102 (2021).